0273-2289/98/70–72—0579$11.50

Phenomenological and Neural-Network Modeling of Cephalosporin C Production Bioprocess

A. J. G. Cruz, M. L. G. C. Araujo, R. C. Giordano, and C. O. Hokka*

Departamento de Engenharia Química, Universidade Federal de São Carlos C. P. 676 - CEP 13565-905, São Carlos, SP, Brazil

ABSTRACT

Cephalosporin C production process with *Cephalosporium acremonium* ATCC 48272 in synthetic medium was investigated and the experimental results allowed the development of a mathematical model describing the process behavior. The model was able to explain fairly well the diauxic phenomenon, higher growth rate during the glucose-consumption phase, and the production occurring only in the sucrose-consumption phase.

Moreover, the process was simulated utilizing the neural-networks technique. Two feed-forward neural-networks with one hidden layer were employed. Both models, phenomenological and neural-networks based, satisfactorily describe the bioprocess. The difficulties in determining kinetic parameters are avoided when neural networks are utilized.

Index Entries: *Cephalosporium acremonium;* cephalosporin C, phenomenological modeling; neural network; diauxic phenomenon.

INTRODUCTION

Cephalosporin C is a β-lactam antibiotic usually produced by *Cephalosporium acremonium* in aerated and agitated tanks. They are *N*-acylated derivatives of 7-aminocephalosporanic acid (7-ACA), which is derived from the cephem nucleus. A cephem is the bicyclic ring system obtained by the fusion of a β-lactam ring with dihydrothiazine ring *(1)*. This natural product is modified by chemical or enzymatic methods to yield the semisynthetic cephalosporins, presently on a grand scale in the pharmaceutical market.

* Author to whom all correspondence and reprint requests should be addressed. E-mail: hokka@power.ufscar.br.

Cephalosporin C is a typical secondary metabolite and its production process presents two distinct phases. In the first phase, denominated trophophase, most growth takes place and an easily metabolized carbon source, normally glucose, is consumed. Throughout this step, low production rates are observed owing to a catabolite repression mechanism blocking the specific enzyme synthesis, as reported by Behmer and Demain *(2)*. When the glucose is exhausted, the idiophase commences. In this phase a second carbon source, usually less easily assimilated, like sucrose, is consumed, promoting the synthesis of specific enzymes that allow higher production rates of the antibiotic. Typical diauxic phenomena are observed concerning these two carbohydrates consumption.

Because of its industrial and therapeutic importance, the cephalosporin C production process is the object of study of many research groups. Matsumura et al. *(3)* have proposed a kinetic model of the production process by *C. acremonium* ATCC 36225 (CW19). These authors have observed drastic microorganism morphological differentiation during the process time, and concluded that a certain morphology was closely associated with the production capability of the strain. They also confirmed the important role of endogenous methionine in antibiotic production and the catabolite repression by glucose. Chu and Constantinides *(4)* have studied this process and have developed a kinetic model aiming at the maximization of this antibiotic production by strains of *C. acremonium* (CW19), applying Pontryagin's maximum principle.

Nowadays the neural-networks approach is becoming popular among researchers to model many chemical and biochemical processes. The first studies in this field started in the earlier 1930s, but it was only in the 1980s that interest in the field reemerged with the publication of the back-propagation algorithm by Rumelhart et al. *(5)*, which has established the feed-forward layered network as the major paradigm of the field.

Thibault et al. *(6)* have investigated the use of neural-network methodology for the modeling of a bioprocess dynamics and prediction of its variables. Di Massimo et al. *(7)* have reported a methodology employing neural-network techniques to infer offline assay information (primary process variables such as cellular and product concentration) with available on-line measurements. Syu and Tsao *(8)* have used neural networks in modeling batch microbial cell growth. In recent studies, Cruz et al. *(9,10)* employed this technique showing very promising results in monitoring, fault detection, and simulation of penicillin-G production bioprocess. The nonlinear behavior of the bioprocess was described satisfactorily by neural-network, and good results obtained by the authors have encouraged the study of this approach in bioprocess modeling and simulation.

In this work, experimental runs for the process were performed and the time course of cell growth, cephalosporin C production, glucose and sucrose consumption were followed during 144–166 h. For the process modeling, two approaches were utilized.

In the phenomenological approach, although the simplifying assumptions regarding the bioprocess kinetics were used, still the problem of large number of parameters to be optimized remained. To avoid this problem, the neural network approach for the bioprocess simulation was utilized by applying two feed-forward neural-networks.

MATERIALS AND METHODS

Microorganism

The strain *Cephalosporium acremonium* ATCC 48272 kindly provided by Fundação Tropical de Pesquisa e Tecnologia "André Tosello" (Campinas, SP, Brazil) was used throughout this work. This strain is able to produce more than 1000 mg cephalosporin C/L, when grown in a synthetic medium and it was kept on agar slants as proposed by Shen et al. *(11)*.

Culture media

For inoculum preparation, a synthetic medium was utilized containing (in g/L): glucose, 30.0; ammonium acetate, 8.8; *DL*-methionine, 5.0; oleic acid, 1.5; KH_2PO_4, 2.3; K_2HPO_4, 5.8; $Fe(NH_4)_2(SO_4)_2/6H_2O$, 0.16; micronutrients were provided by salt solution addition (50 mL/L). Its composition was in (g/L): Na_2SO_4, 16.2, $MgSO_4 \cdot 7H_2O$, 7.68, $CaCl_2 \cdot 2H_2O$, 1.6, $MnSO_4 H_2O$, 0.64, $ZnSO_4 \cdot 7H_2O$, 0.64, $CuSO_4 \cdot 5H_2O$, 0.04. The production medium contained (in g/L): glucose, 27.0; sucrose, 36.0; the other components were the same as the inoculum medium. The media compositions were similar to that utilized by Demain et al. *(12)*. In the case of glucose-phase parameter evaluation, sucrose was not added.

Experimental Procedure

The cell spores from agar slants were transferred to preculture medium in 250 mL shake flasks and incubated for 48 h 250 rpm at 26°C. After spore germination, a new preculture was carried out for 24 h at same conditions. The cultivated cells were then used to inoculate the main fermentation broth with free cells. The main experiments were carried out in 250-mL shake flasks, at 26°C and agitation speed of 250 rpm. The seed was 10% in volume. Runs were carried out for 144–166 h and samples were taken periodically for cell mass, the sugars, and cephalosporin C concentration.

Analysis

The cell-mass concentration was evaluated as dry weight at 105°C, in g/L. Glucose was measured utilizing enzymatic GOD-PAP method *(13)* and sucrose was measured by the same method, following acid hydrolysis. Cephalosporin C titers were determined by an agar diffusion bioassay *(14)* utilizing *Alcaligenes faecalis* ATCC 8750.

PHENOMENOLOGICAL APPROACH

Kinetic Model

The kinetic model developed was based on stoichiometric equations, representing the main steps in cell, substrates, oxygen, and product variation. In these equations, only the limiting substrate, cell, oxygen, and product are represented since the other nutrients are considered to be in excess.

The total biomass was assumed to be composed of cells X_1, submitted to catabolite repression by glucose S_1, during the growth phase (Eq. 1), and cells X_2, derepressed after glucose depletion and capable of consuming sucrose S_2 (Eq. 4). Repression and derepression refer to the regulatory mechanism of formation of the enzyme complex responsible for the cephalosporin synthesis. In glucose concentration lower than a certain critical value, Cs_{c1} (1.5 g/l), cells X_1 are transformed into cells X_2 (Eq. 3).

$$aO_2 + S_1 + X_1 \rightarrow (1 + Y_{xs1})X_1 + Y_{px1}P \quad (1)$$

$$bO_2 + X_1 \rightarrow D_1 \quad (2)$$

$$X_1 \rightarrow X_2 \quad (3)$$

$$cO_2 + S_2 + X_2 \rightarrow (1 + Y_{xs2})X_2 + Y_{px2}P \quad (4)$$

$$dO_2 + S_2 \xrightarrow{X_2} Y_{px3}P \quad (5)$$

$$eO_2 + X_2 \rightarrow D_2 \quad (6)$$

$$P \rightarrow D_3 \quad (7)$$

where total cell mass (X) includes both types of cells, defined as X_1 and X_2, D_1 and D_2 are products of cell degradation, during the glucose (S_1) and sucrose (S_2) consumption phase, respectively; and D_3 is the degradation product of P.

Rate Equations

Rate equations related to the above mentioned stoichiometric equations describing the behavior of the process were based on those proposed by Araujo et al. *(15)* as follows:

$$Rx_1 = \frac{dCx_1}{dt} = \left\{\left[\left(\frac{\mu_{max1}Cs_1}{k_{x1}Cx_1 + Cs_1}\right)\cdot\left(\frac{C_{O2}}{k_{O2} + C_{O2}}\right)\right] - k_{d1}\right\}Cx_1 - \left[\frac{(k_TCx_1)}{(k_1 + Cx_1)}\right] \quad (8)$$

$$Rx_2 = \frac{dCx_2}{dt} = \left\{\left[\left(\frac{\mu_{max2}Cs_2}{k_{s2} + Cs_2 + K_iCs_2^2}\right)\cdot\left(\frac{C_{O2}}{k_{O2} + C_{O2}}\right)\right] - k_{d2}\right\}Cx_2 + \left[\frac{(k_TCx_1)}{(k_1 + Cx_1)}\right] \quad (9)$$

$$Rs_1 = \frac{dCs_1}{dt} = -\left[\left(\frac{1}{Y_{xs1}}\right)\cdot\left(\frac{\mu_{max1}Cs_1}{k_{x1}Cx_1 + Cs_1}\right)\cdot\left(\frac{C_{O2}}{k_{O2} + C_{O2}}\right)\right]Cx_1 \tag{10}$$

$$Rs_2 = \frac{dCs_2}{dt} = -\left\{\left[\left(\frac{1}{Y_{xs2}}\right)\cdot\left(\frac{\mu_{max2}Cs_2}{k_{s2} + Cs_2 + K_iCs_2^2} + m\right)\cdot\left[\left(\frac{C_{O2}}{(k_{O2} + C_{O2})}\right)\right]\right\}Cx_2 \tag{11}$$

$$Rc_P = \frac{dCp}{dt} = \left[\left[\left\{\frac{Y_{px1}}{Y_{xs1}}\cdot\left[\frac{(\mu_{max1}Cs_1)}{(k_{x1} + Cs_1)}\right]\right\}Cx_1 + \left\{\left(\frac{Y_{px2}}{Y_{xs2}}\right)\cdot\left[\frac{(\mu_{max2}Cs_2)}{(k_{s2} + Cs_2 + K_iCs_2^2)}\right] + Y_{px3}\cdot m\right\}Cx_2\right]\right]\cdot\left[\frac{C_{O2}}{(k_{O2} + C_{O2})}\right] \tag{12}$$

$$Rc_{O2} = \frac{dC_{O2}}{dt} = k_La(C^*_{O2} - C_{O2}) - \left[\frac{(R_{max}\cdot C_{O2})}{(k_{O2} + C_{O2})}\right] \tag{13}$$

The first term in Eqs. 8 and 9 represents growth of cells due to glucose and sucrose substrate sources. The second terms refer to the transformation of repressed cells into derepressed ones. Equation 10 is the glucose consumption rate, assuming that this substrate is used only for growth, whereas Eq. 11 represents sucrose consumption rate. The production rate is describe by Eq. 12, with three terms, related to the growth in glucose, and growth and maintenance in sucrose. Each of these terms appears associated with yield factors (or pseudo stoichiometric coefficients) Y_{Px1}, Y_{Px2} and Y_{Px3}, respectively. Equation 13 represents the time course of dissolved oxygen during the process.

Sucrose is slowly consumed during the process low activity of sucrose hydrolyzing enzyme; in this phase little cell growth is observed. Therefore in this phase it has been assumed that the process was limited by enzyme activity both in growth and maintenance reactions.

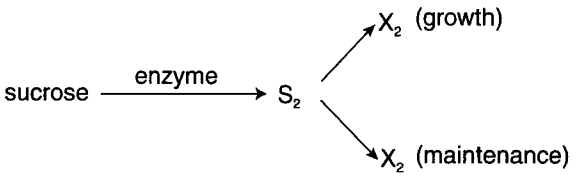

and Eq. 11 becomes:

$$Rs_2 = \frac{dCs_2}{dt} = -\left[\left(\frac{1}{Y_{x2}}\right)\cdot\left(\frac{\mu_{max2}Cs_2}{k_{s2} + Cs_2 + K_iCs_2^2}\right)\cdot\frac{C_{O2}}{k_{O2} + C_{O2}}\right]Cx_2 \tag{14}$$

where:

$$\frac{1}{Y_{x2}} = \frac{1}{Y_{xs2}} + \frac{m}{\mu_{max2}}$$

where Y_{x2} is an overall yield coefficient which includes the amount of sucrose used by the microorganisms in growth and maintenance.

With this assumption in sucrose kinetics, the product equation becomes:

$$Rc_P = \frac{dCp}{dt} = \left[\left(\left(\frac{Y_{px1}}{Y_{xs1}} \cdot \frac{\mu_{max1} Cs_1}{k_{x1} + Cs_1}\right)\right) Cx_1 + \left(\left(\frac{Y_{px2}}{Y_{x2}}\right) \cdot \left(\frac{\mu_{max2} Cs_2}{k_{s2} + Cs_2 + K_i Cs_2^2}\right)\right) Cx_2\right] \cdot \frac{C_{O2}}{k_{O2} + C_{O2}} \quad (15)$$

These equations were solved numerically using the Differential-Algebraic system solver (DASSL) algorithm developed by Petzold *(16)*, in a 486 DX-4, 100-MHz microcomputer. The estimation of model parameters was carried out following a nonlinear least square approach, using the Marquardt method *(17)*.

NEURAL-NETWORK APPROACH

Two feed-forward neural-networks (FNN) were employed in this work to estimate cell and antibiotic concentration. The two nets were described in Fig. 1, and consist of one input layer, one output layer, and one hidden layer. The activation function employed was sigmoidal *(18)*. The objective function of choice for the minimization criterion in the training algorithm was the mean square error between the neural output and the desired output from all the input pattern in the data base, given by:

$$\text{Obj\_f} = \sum_p E_p \quad (16)$$

where E_p is:

$$E_p = \frac{1}{2} \|Y_p - d_p\|^2 \quad (17)$$

where y_p: value obtained from neural network, d_p: desired value from data base.

The first FNN had three hidden neurons, and an input with three variables: ($C_{s1}[k]$, $C_{s2}[k]$, $C_x[k]$), where k is the present time. The output vector was cell concentration in future time ($C_x[k + 1]$).

The second FNN was used to estimate antibiotic concentration in future time ($C_p[k + 1]$), and had four hidden neurons. Its input was composed of three variables ($C_{s1}[k]$, $C_{s2}[k]$, and $C_x[k]$) in present time.

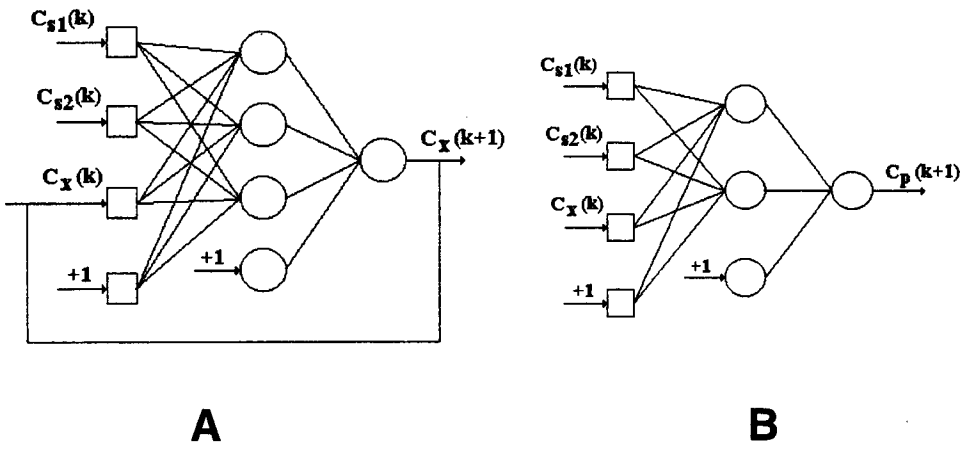

Fig. 1. Basic feed-forward neural-network architecture (FNN): **(A)** the first FNN, used to estimated cell concentration; **(B)** the second FNN, employed to infer antibiotic concentration.

Data Base

The data used to train the two FNN were obtained from 14 sets of experimental data.

RESULTS AND DISCUSSION

Parameters Estimation: Phenomenological Approach

Growth of the microorganism in a medium with glucose as the major carbon source was carried out to determine the parameters of the equation proposed by Contois *(19)*. This model was preferred as at high cell concentrations, serious diffusional limitations can be expected. This model has been utilized by Bajpai and Reuss *(20)* for describing *Penicillium chrysogenum* growth. In Fig. 2, a good fit is shown between experimental data and the model. Parameters μ_{max1}, k_x and Y_{xs1} were estimated by nonlinear regression for this experiment *(17)*; their values are shown in Table 1.

For the sucrose-utilizing phase, the study was carried out in a medium containing glucose and sucrose as major carbon sources, and the samples were taken after 48 fermentation, when it was assumed that the glucose was already depleted. Figure 3 depicts the experimental data and calculated results. Parameters μ_{max2}, k_{s2}, K_i, k_{d2}, and Y_{x2} were estimated using the Marquardt method as shown in Table 1.

Regarding the respiration rate, the influence of sucrose or glucose concentration was investigated by Araujo *(21)*, and specific respiration rate during this process was shown to be independent of sugar type or concentration. The specific respiration rate behaves as a zero-order reaction

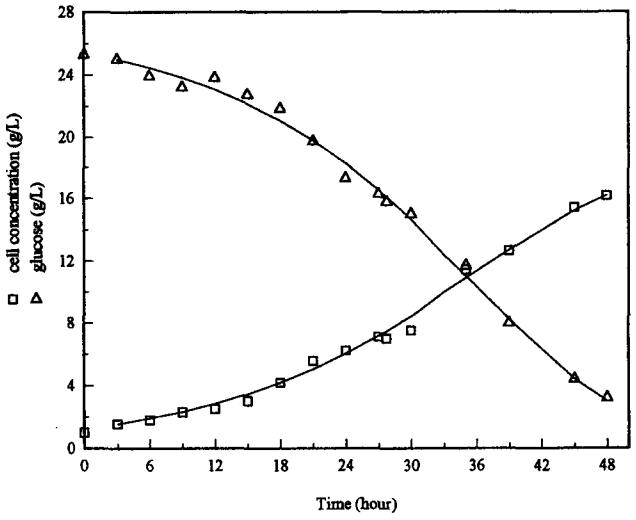

Fig. 2. Experimental data of cephalosporin C fermentation and fit of the kinetic model proposed to growth phase in glucose.

Table 1
Estimated Parameters, with 95% Confidences Intervals, Used for Simulation of Cephalosporin C Production Process by *C. acremonium* ATCC 48272 in Shake Flasks

Maximum specific growth rates	μ_{max1}	0.0671 ± 0.0029 (h^{-1})
	μ_{max2}	0.0364 ± 0.0143 (h^{-1})
Contois constant	k_{x1}	0.379 ± 0.122 (gS_1/gX_1)
saturation constant	k_{s2}	12.0 (gS_2/L)
inhibition constant	K_i	0.154 ± 0.105 $(gS_2/L)^{-1}$
death rate constant	k_{d2}	0.006 (h^{-1})
	k_{d3}	0.0015 (h^{-1})
yield coefficients (sugar consumption)	Y_{xs}	0.599 ± 0.028 (gX_1/gS_1)
	Y_{x2}	0.399 ± 0.04 (gX_2/gS_2)
yield coefficients (product formation)	Y_{px1}	0.0045 (gP/gX_1)
	Y_{px2}	0.035 (gP/gX_2)
kinetic constants	k_T	6.0 ($gX_1/L/h$)
	k_1	0.01 (gX_1/L)
maximum specific respiration rate	R_{max}	1.055 ± 0.219 $mmolO_2/gX/h$)
kinetic constant (respiration rate)	k_{O2}	0.00277 ± 0.00073 ($mmolO_2/L$)
volumetric gas-liquid mass transfer coefficient	k_La	162.0 (h^{-1})
oxygen saturation concentration	C_{O2}^*	0.22 ($mmolO_2/L$)
critical value of glucose concentration	C_{slc}	1.5 (gS_1/L)

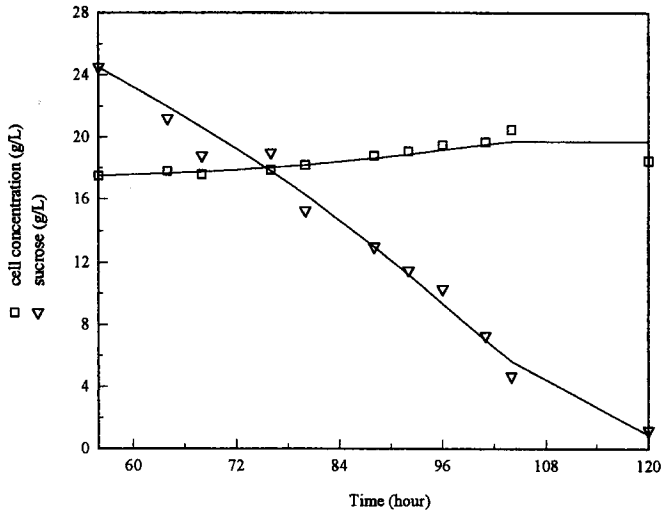

Fig. 3. Experimental and calculated data of the cephalosporin C bioprocess during sucrose consumption phase.

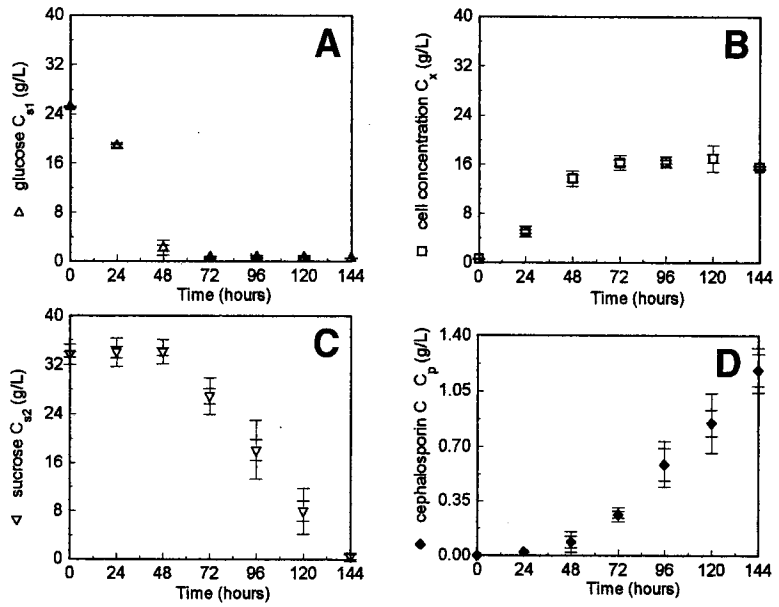

Fig. 4. Plot of **(A)** glucose, **(B)** sucrose, **(C)** cell and **(D)** cephalosporin C concentrations during the time course of the bioprocess. Variance and standard deviation were presented for the median values of the variables.

for both sugars. The author also measured R_{max} and k_{O2} considering that kinetics concerns oxygen concentration. The values adopted in this work are shown in Table 1.

Fourteen sets of experimental data were collected. Figure 4 presents the values of glucose, sucrose, cell, and cephalosporin C concentrations

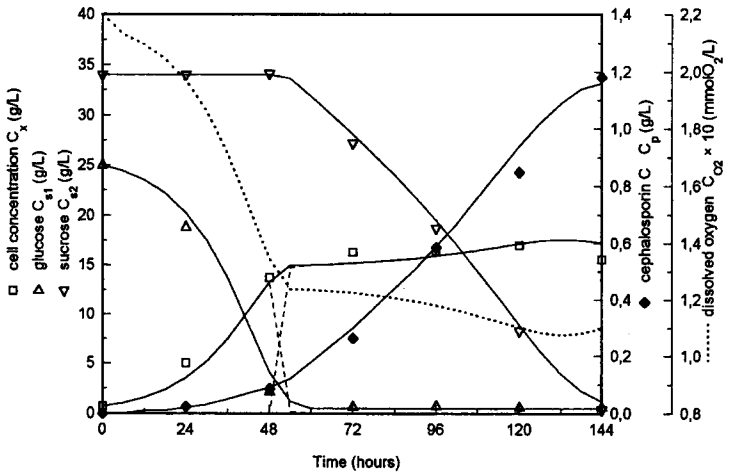

Fig. 5. Simulated results and experimental data of cephalosporin C production process by *C. acremonium* ATCC 48272 in shake flasks.

during the time course of the bioprocess. The data presented represent the average values for the 14 experimental runs.

For the remaining parameter values, the differential equation sets were solved numerically and the set of the constant values were optimized by nonlinear, least-square regression analysis following Marquadt's procedure. The values so determined are shown in Table 1.

Calculated values obtained by simulating the model are shown in Fig. 5. As can be observed, the proposed model explains very well the complex features of this bioprocess, such as diauxic growth and the higher production rate taking place mostly during the sucrose consumption phase.

A volumetric oxygen transfer coefficient was determined for this experiment. Also, dissolved oxygen behavior was simulated, and it was established that its concentration, though dropping at the beginning of cultivation in the growth phase, did not fall below 45%.

Cephalosporin C specific production rate was approx 0.53 mg/g cell/h, considering the whole process time.

Neural-Network Training

The neural-network was trained by successive presentations of input-output data pairs from the database. Three different algorithms were tested: classical back propagation *(5)*, random search procedure (RSP) *(7)*, and a mixed procedure combining the last two procedures *(22)*. The second approach was most efficient in this case.

A comparison between back propagation and random search training procedures was made; the results are shown in Fig. 6. The solid line repre-

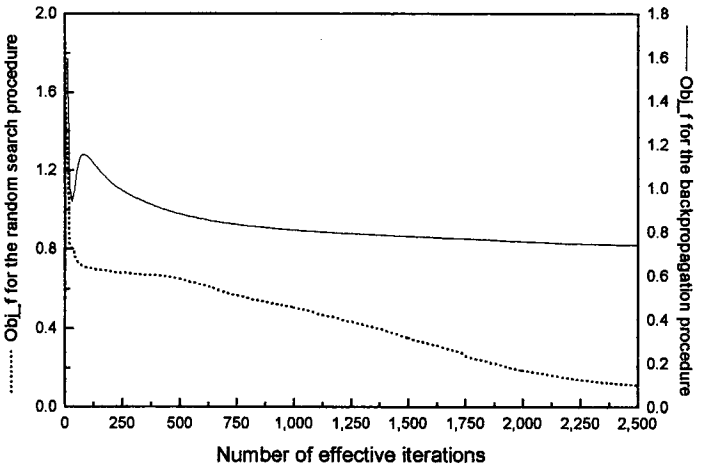

Fig. 6. Plot of error criterion for minimization of objective function based on random search algorithm and error criterion for minimization of objective function based on back propagation algorithm.

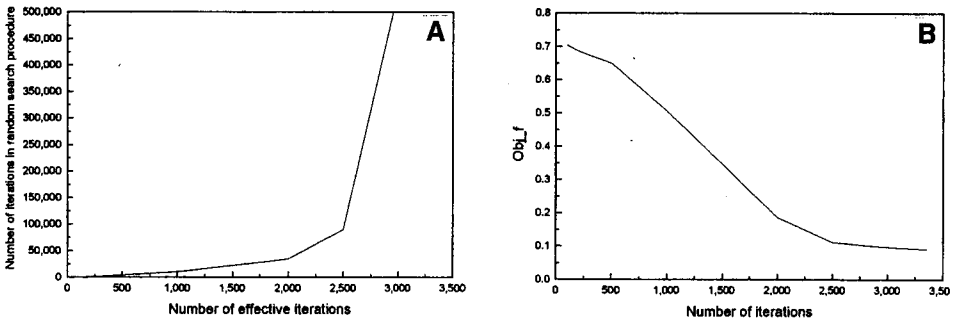

Fig. 7. **(A)** Number of effective iterations vs number of iterations in RSP algorithm; **(B)** number of iterations vs objective function values.

sents the value of objective function for the back propagation algorithm, whereas the dashed line shows its value for the random search algorithm.

In Fig. 6 only the number of effective iterations for the random search algorithm was considered. It is evident that the random search procedure is much more efficient and robust, whereas the classical backpropagation method shows a tendency to stabilize toward a local minimum.

To determine the number of iterations to be used to stop the training algorithm, the behavior of the number of iterations in RSP and the value of objective function in relation to the number of effective iterations was examined. Figure 7A, B depicts the results.

Figure 7A shows that by increasing the number of effective iterations in the random search procedure, the number of iterations become excessively high and, as a consequence, the processing time lengthens to a point

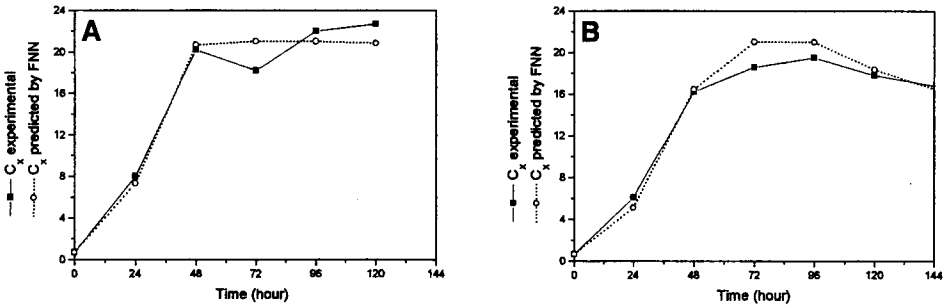

Fig. 8. Simulation results from 3 × 3 × 1 FNN: **(A)** C_{s1} = 25 g/L, C_{s2} = 36 g/L, and C_{x1} = 0.7 g/L initial conditions; **(B)** C_{s1} = 25.4 g/L, C_{s2} = 36 g/L, and C_{x1} = 0.65 g/L initial conditions.

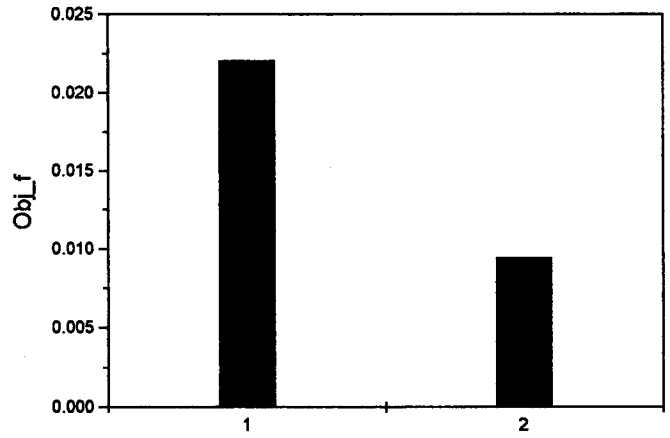

Fig. 9. Comparison between the back propagation and random-search training algorithms for 300 effective iterations.

where it becomes useless, since objective function value does not decrease significantly only above 2500 iterations, as shown by Fig. 7B. Therefore, this number of iterations was adopted as the end value for the network training process.

The neural network described in Figs. 1A, B were employed to infer the cell and cephalosporin C concentration, respectively. Figs. 8A, B show two different simulations. Figure 8A exemplifies the accuracy of the network fitting to a set of data used in the training procedure.

The good agreement is in fact already expected, because of the well-known capability of these algorithms to forecast nonlinear behaviors. Fig. 8B, on the other hand, shows an example of the FNN ability to forecast the general trend of the system, in a situation not used during the training phase. In the case depicted in Fig. 8B, the initial cell concentration is 7.14% less than in Fig. 8A (from 0.65 against 0.7 g/L). This is a typical variation

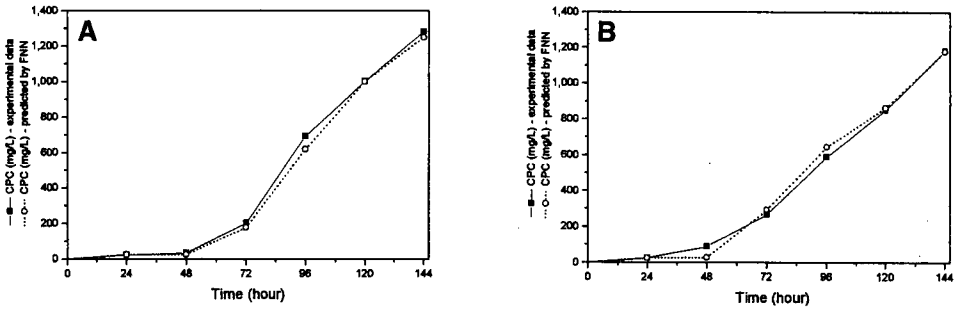

Fig. 10. Simulation results from 3 × 2 × 1 FNN: **(A)** Initial conditions: C_{s1} = 25.4 g/L; C_{s2} = 36 g/L; C_x = 0.65 g/L **(B)** Initial conditions: C_{s1} = 25 g/L; C_{s2} = 34 g/L; C_x = 0.7 g/L.

in this kind of experiment, and the FNN is able to follow the empirical observations.

For cephalosporin C estimation, sucrose, glucose and mass concentration obtained from the database were used as network inputs, whereas the cephalosporin C concentration is the network output. Best results were obtained using RSP algorithm, as depicted in Fig. 9.

Figure 10 illustrates the simulation by this technique of the cephalosporin C time course. Two data sets not used during the training are displayed in this figure; in both cases an excellent fitting to the experimental values can be noticed.

Thus, for a complex biological process, this technique is demonstrated to be very useful and promising for control and optimization when coupled with data acquisition systems.

CONCLUSIONS

The phenomenological model proposed here satisfactorily describes the main features of this bioprocess, such as diauxic effect, different sugar consumption rates and antibiotic production during the second phase.

The inherent difficulties when estimating a large number of adjustable parameters in the phenomenological approach were avoided when the neural-network approach was used.

Indeed, the neural-network method is a promising alternative to circumvent time delay in measuring cell mass and cephalosporin C concentration. Consequently, more robust control strategies are about to appear on the horizon.

Studies utilizing this technique are presently being performed in our laboratories, and indicate that this approach should be highly valuable for improvements in this process when combined with online measurements. Particularly the FNN in Fig. 1A uses only initial cell concentration to predict the cellular mass during the hole process. This feature may be useful

to infer the trend of important online variables that are measured offline in the real process, such as cell and antibiotic concentrations.

ACKNOWLEDGMENTS

The authors gratefully acknowledge the financial support of CAPES (Ministry of Education Brazil), and scholarship from FAPESP (São Paulo State Foundation, Brazil) for two of the authors (A.J.G.C. and M.L.G.C.A.). The English review by Paula Matvienko-Sikar is also acknowledged.

REFERENCES

1. El-Sayed, A.-H. M. M. (1992), in *Handbook of Applied Mycology*, vol. 4, Arora, D. K., ed., Banaras Hindu University, Varanasi, India, pp. 517–564.
2. Behmer, C. J. and Demain, A. L. (1983), *Current Microbiol.* **8,** 107–114.
3. Matsumura, M., Imanaka, T., Yoshida, T., and Taguchi, H. (1981), *J. Ferment. Technol.* **59(2),** 115–123.
4. Chu, W. B. Z and Constantinides, A. (1988), *Biotechnol. Bioeng.* **32,** 277–288.
5. Rumelhart, D. E. and McClelland, J. L. (1986), in *Parallel Distributed Processing: explorations in the microstructure of cognition*, vol. 1, MIT, Cambridge, MA, pp. 318–362.
6. Thibault, J., Breusegem, Van V., and Chéruy, A. (1990), *Biotechnol. Bioeng.* **36,** 1041–1048.
7. DiMassimo, C., Montague, G. A., Willis, M. J., Tham, M. T., and Morris, A. J. (1992), *Computers Chem. Eng.* **16(4),** 283–291.
8. Syu, M.-J and Tsao, G. T. (1993), *Biotechnol. Bioeng.* **42,** 376–380.
9. Cruz, A. J. G., Hokka, C. O., and Giordano, R. C. (1996), *Proceedings of the 11st Simpósio Nacional de Fermentações (XI SINAFERM, São Carlos, SP, Brasil)*, **1,** pp. 84–89.
10. Cruz, A. J. G, Hokka, C. O., and Giordano, R. C. (1996), *Proceedings of the 3rd Congreso Interamericano de Computacion Aplicada a la Industria de Procesos (CAIP '96, Villa Maria, Cordoba, Republica da Argentina)*, pp. 115–118.
11. Shen, Y.-Q, Wolfe, S., and Demain, A. L. (1986), *Bioeng. Biotechnol.* **4,** 61–63.
12. Demain, A. L., Newkirk, J. F., and Hendlin, D. (1963), *J. Bacteriol.* **85,** 339–344.
13. Barham, D. and Trinder, P. (1972), Analyst, **97(2),** 142–145.
14. Claridge, C. A. and Johnson, D. L. (1962), *Antimicrobiol. Ag. Chemother.* 682–686.
15. Araujo, M. L. G. C., Oliveira, R. P., Giordano, R. C., and Hokka, C. O. (1996), *Chem. Eng. Sci.* **51(11),** 2835–2840.
16. Petzold, L. (1989), Subroutine DDASSL, Computing and Mathematics Research Division, Lawrence Livermore National Laboratory, Livermore, CA.
17. Marquardt, D. W. (1963), *J. Soc. Indust. Appl. Math.* **11,** 431–441.
18. Bhat, N. and McAvoy, T. J. (1990), *Computers Chem. Eng.* **14(4/5),** 573–583.
19. Bailey, J. E. and Ollis, D. F. (1986), *Biochemical Engineering Fundamentals*, 2nd ed., McGraw-Hill, New York.
20. Bajpai, R. K. and Reuss, M. (1981), *Biotechnol. Bioeng.* **22,** 739–763.
21. Araujo, M. L. G. C. (1996), *PhD Thesis*, Chemical Engineering Department, Federal University of São Carlos, SP, Brazil.
22. Cruz, A. J. G. and Giordano, R. C. (1996), *Proceedings of the 11st Brazilian Congress of Chemical Engineering (11 COBEQ, Rio de Janeiro, RJ)*, 571–576.